BMC Medical Imaging

RESEARCH

Open Access

Fractional differentiation based image enhancement for automatic detection of malignant melanoma

Basmah Anber[1*] and Kamil Yurtkan[1,2]

Abstract

Recent improvements in artificial intelligence and computer vision make it possible to automatically detect abnormalities in medical images. Skin lesions are one broad class of them. There are types of lesions that cause skin cancer, again with several types. Melanoma is one of the deadliest types of skin cancer. Its early diagnosis is at utmost importance. The treatments are greatly aided with artificial intelligence by the quick and precise diagnosis of these conditions. The identification and delineation of boundaries inside skin lesions have shown promise when using the basic image processing approaches for edge detection. Further enhancements regarding edge detections are possible. In this paper, the use of fractional differentiation for improved edge detection is explored on the application of skin lesion detection. A framework based on fractional differential filters for edge detection in skin lesion images is proposed that can improve automatic detection rate of malignant melanoma. The derived images are used to enhance the input images. Obtained images then undergo a classification process based on deep learning. A well-studied dataset of HAM10000 is used in the experiments. The system achieves 81.04% accuracy with EfficientNet model using the proposed fractional derivative based enhancements whereas accuracies are around 77.94% when using original images. In almost all the experiments, the enhanced images improved the accuracy. The results show that the proposed method improves the recognition performance.

Keywords Edge detection, Fractional differentiation, Grunwald Letnikov, Melanoma, Deep learning

Introduction

Digital image processing is a constantly evolving field of research that is interrelated with other disciplines such as mathematics, computing, and human perception and image manipulation. Advancements in hardware and programming languages have made it possible to apply mathematical methods in various applications, including medicine, biology, archeology, geology, and astronomy. Edge detection is a vital component of image processing that involves identifying the boundaries between regions of varying gray levels in an image. These edges provide valuable information about objects and help in tasks such as object recognition and region segmentation. Numerous mathematical algorithms have been developed for edge detection, including first-order differential algorithms. For instance, the edge detection method was used in [1] to remove speckle noise while preserving diagnostic information in images, while [2] used the Canny and Sobel algorithms. In [3], the Sobel edge detection algorithm was used to analyze radar remote sensing images, and [4] applied the Roberts edge detector on both gray

*Correspondence:
Basmah Anber
basmaanber2@gmail.com
[1]Computer Engineering Department, Faculty of Engineering, Cyprus International University, via Mersin10, Nicosia, Northern Cyprus, Turkey
[2]Artificial Intelligence Application and Research Center, Cyprus International University, via Mersin10, Nicosia, Northern Cyprus, Turkey

and color images. However, these techniques can produce thick edges with poor detection quality.

Besides the use of computer vision, the machine learning (ML) and deep learning (DL) methods are well employed in automatic medical analysis. The study given in [5] uses machine learning algorithms to understand pharmaceutical permeability via the placenta, ensuring safety for both mother and unborn chil. DL has the potential to revolutionize neurological disease treatment by enabling drugs to cross the blood-brain barrier (BBB) [6]. DL has significantly improved the accuracy of estimating gender and age from ECG data over the past decade [7]. This expertise is crucial for creating personalized medical treatments and preventative measures, revolutionizing other biological research areas and demonstrating its potential for estimating gender and age from ECG data [8]. DL's non-invasive, effective, and precise instrument is crucial for future healthcare developments [9].

In image processing and computer vision, using identified edges to improve images is a frequent practice. Edge detection is a key stage in image analysis that includes locating the borders or transitions between various sections in an image. These borders frequently correspond to noticeable alterations in hue or intensity, which can convey crucial details about the boundaries and forms of objects in the image. Once the edges are found, they may be utilized in a number of ways to improve the image's quality, which will affect the detection process as well. Edge detection helps eliminate irrelevant information, reducing the size of the image while preserving its structural properties.

Edge detection in color images presents a greater challenge than in grayscale images due to the vector definition of color images, which consists of three components (red, green, and blue) assigned to each pixel. While a discontinuity in intensity is considered an edge in grayscale images, it is not precisely defined in color images. It can be considered an edge in a color image if there is a discontinuity in the intensity of one of its channels.

One of the main challenges that edge detection faces is textural variability, making it challenging for edge detection algorithms to accurately capture the lesion boundaries [10, 11]. Skin lesions can exhibit a wide range of colors, making it difficult for edge detection methods to identify the lesion boundary [12]. Skin lesion images can contain significant background noise, such as hair, wrinkles, and other non-lesion structures, which can interfere with the edge detection process [13, 14]. In addition, changes in illumination can affect the appearance of skin lesion images, making it difficult for edge detection algorithms to accurately identify the lesion boundary [15].

Edge detection is a fascinating field in image processing, driven by the idea of using the Grunwald-Letnikov definition, a non-integer differential, to detect edges. The application of non-integer differentials in image processing, including edge detection, is a cutting-edge technique that is currently being explored by many researchers to enhance existing image processing methods and expand into other areas as well. The advantages of using edge detection with non-integer differentials include the ability to easily modify the order of derivation, resulting in improved edge detection outcomes, and the simplicity of the algorithms used. The goal of this study is to demonstrate that the Grunwald-Letnikov definition satisfies these requirements and offers even more benefits in edge detection.

Medical imaging uses high-resolution images for diagnosis and treatment of various medical issues. ConvUNeXt, a convolutional neural network, improves precision and efficacy in medical image segmentation [16]. Liver Computerized Tomography (CT) segmentation uses a small neural network using multiscale feature augmentation for accurate identification of liver structures and diseases [17]. DRU-Net, a deep convolutional neural network, solves common problems in medical imaging, such as objects, noise, and artifacts [18]. Dense-PSP-UNet optimizes liver ultrasound segmentation, integrating dense connection patterns with U-Net structures and pyramid scene parsing [19]. CoTr, a groundbreaking 3-Dimensional (3D) medical imaging technique, combines convolutional neural networks with transformers to segment 3D images [20]. Accurate segmentation using Magnetic Resonance Imaging (MRI) and CT images enhances safety, effectiveness, and patient outcomes [21]. Fusion imaging outperforms single-modality imaging for rapid post-ablation evaluation of malignant liver neoplasms [22, 23]. Deep learning techniques improve B-mode ultrasound segmentation, enabling accurate delineation of anatomical structures and diseased areas [24].

In this study, the classification abilities of EfficientNetv2 models are examined on the HAM10000 dataset with the use of proposed image enhancement technique, of dermatoscopic images [16, 17]. The collection includes 10,015 images from seven types of skin cancer: Actinic keratoses and intraepithelial carcinoma (akiec), basal cell carcinoma (bcc), seborrheic keratoses and lichen-planus (bkl), dermatofibroma (df), melanoma (mel), melanocytic nevi (nv), and vascular lesions (vasc). Transfer learning and Convolutional Neural Networks (CNN) fine-tuning for the HAM10000 dataset were accomplished using ImageNet pre-trained weights.

In this paper, our main objective is to enhance the image quality with fractional differentiations in order to robustly detect skin lesions causing melanoma. We can list our objectives as:

- Enrich the use of fractional derivatives in edge detection to include different frequencies that first and second derivatives cannot detect.
- Use enhanced images with fractional derivatives to provide robust image representation.
- Improve the accuracy of automatic detection of skin lesions causing melanoma through enhanced images by using deep learning.
- Experimentally compare the performance of the enhanced images with the original images.

The structure of the paper is as follows: The paper starts with the introduction, including the motivations for the study. Then a brief literature review is given in the second section, titled Related Work. The methodology is explained in details in Sect. 3. Section 4 presents experimental results. Finally, the paper is concludes with the conclusion section.

Related work

Fractional differentiation, also known as non-integer differentiation, has a long history dating back to 19th-century mathematicians and physicists such as Cauchy, Riemann, Liouville, and Letnikov. Since then, various mathematicians and physicists have explored fractional differentiation equations, particularly fractional-order linear differentiation equations. There are numerous works that delve into the mathematical study of these equations, such as [18, 19, 25, 26]. In recent years, fractional differentiation has become increasingly important in fields such as mechanics, electricity, chemistry, biology, economics, modeling, system identification in time and frequency domain control theory, mechatronics, and robotics [18, 27]. This study also utilized fractal image compression [5, 28–32].

In an effort to achieve efficient edge detection with good localization and minimal response, the Canny edge detector was developed using the calculus of variations. This technique optimizes a given function to produce the optimal function, which is defined as the sum of four exponential terms. However, this optimal function can be approximated by the first derivative of a Gaussian [33].

The Sobel operator calculates an approximation of the gradient of the image intensity at each pixel. The output of the Sobel operator can either be the gradient vector or the magnitude of the image vector at that particular pixel. The Sobel operator is computationally inexpensive due to its use of a small, separable, and integer-valued filter in the horizontal (x) and vertical (y) directions in a convolution operation with the image. However, this results in a relatively rough approximation of the gradient, particularly in the presence of frequent changes in the image's frequency [34].

The Prewitt edge detector is a discrete differentiation operator that estimates the gradient intensity of an image. It works by applying a small, separable, integer-valued filter to the image through convolution in both the horizontal and vertical directions. This operator is efficient and fast at detecting edges, although it is best suited for use with noiseless and high-contrast images [35]. The filter calculates the light intensity gradient at each pixel of the image, showing the direction and rate of the largest change in brightness. The output highlights abrupt changes in the image's brightness and thus reveals the probable edges. This technique is practical, reliable, and simple to implement. The Roberts edge detector relies on the computation of the first derivative of the image [36].

The Marr and Hildreth operator is exclusively used in digital images and searches for zero crossings in the image's second derivative. Multiple methods exist for performing these calculations, including convolution of the image with a Gaussian kernel and approximation of the second derivative (Laplacian method) using a 3×3 mask, or convolution of the image using a mask derived from the Laplacian of Gaussian (LoG) function. The latter can also be achieved through the use of recursive Gaussian filters [37]. To implement the algorithm, two steps are necessary: convolving the image and locating zero crossing points in the filtered image. The image convolution stage can be further divided into two steps: using a LoG kernel or using a Gaussian kernel followed by a Laplacian operator. In the development of the Marr-Hildreth algorithm, a Gaussian kernel, a Laplacian Gaussian kernel, and a 2-D mask are required for convolving the image with a kernel. The concept behind the Gaussian and Laplacian of the Gaussian kernel is to perform a convolution operation on the input image.

The Haralick operator, similar to the Marr-Hildreth operator, aims to locate zero crossing points in the second derivative of an image. However, the Haralick operator uses a local bi-cubic polynomial approximation to smoothly approximate the input image. This analytical computation involves using an equivalent expression to identify zeros of the second derivative of a polynomial function, given its parameters [38].

Edge detection aims to identify key features in an image, such as sharp changes in gray-level values. One of the earliest edge detection methods was the Roberts cross operator, introduced by Roberts [39]. The Prewitt operator employs two kernels that are applied to the image through convolution, allowing for the estimation of derivatives in both horizontal and vertical directions [40]. The Sobel operator, a discrete differentiation operator, is used to approximate the intensity gradient of an image [41, 42]. Image data can also be reduced to a size suitable for edge detection analysis [43]. However, reducing noise is important to maintain image quality and

prevent unexpected results, as the performance of edge detection tasks relies on edge information [44, 45]. Skin cancer classification is the focus of Ali et al.'s research [46], which places special emphasis on EfficientNets' multiclass classification capabilities. Our research delves into a distinct approach by combining neural network designs with fractional differentiation approaches. Our goal is to improve edge recognition in skin lesion images. Despite their common goal of improving skin cancer detection using deep learning techniques, these studies use different methodologies. This shows how important it is to have multiple tactics to handle the difficulties of skin cancer analysis. Popescu et al. [47] looked at skin lesion classification with the use of many neural networks' combined intelligence in their study. Their method improves skin lesion analysis classification performance by using an ensemble of neural networks. On the other hand, we've been working on improving edge recognition in skin lesion pictures by combining fractional differentiation methods with neural network topologies. Despite their differences in methodology, both studies aim to improve skin lesion analysis using modern computational tools. Our approach investigates the integration of fractional differentiation techniques to refine feature extraction and improve classification accuracy, in contrast to Popescu et al.'s emphasis on the collective intelligence of neural networks. These comparisons highlight how different perspectives are crucial for progress in skin lesion categorization and analysis.

Methodology

The proposed method uses fractional derivatives in two different degrees. The fractional derivatives are applied to the input images, and then the resulting images are added to the original images. In the last stage, two deep learning models are employed to train and detect melanoma.

The technique for this investigation comprises many essential components. At first, the main data source is the HAM10000 dataset, which contains dermatoscopic pictures of skin lesions. After that, the pixel values are normalized, the images are resized to a uniform dimension, and noise reduction algorithms are applied to ensure the data is consistent and of good quality. Following the preprocessing, the images are improved by using fractional differentiation according to the Riemann-Liouville (R-L) and Grunwald-Letnikov (G-L) standards. This phase is designed to make lesion borders easier to read and to further standardize the output.

A neural network architecture called EfficientNetV2 is used during the feature extraction and model training phases. The model is trained using preprocessed and augmented pictures. In the classification phase, the trained EfficientNetV2 model is used to assign each image in the dataset to a specific category.

HAM10000 dataset, which contains 10,015 dermatoscopic pictures illustrating seven distinct skin cancer subtypes. Fractional differentiation using the G-L and R-L definitions to improve edge detection.

The proposed method's general block diagram is shown in Fig. 1. The technique is depicted in this graphic in a systematic fashion, beginning with data gathering and preprocessing and progressing through picture improvement, feature extraction, model training, and finally, assessment and classification. The EfficientNetV2 model was used to increase classification accuracy and picture quality, with each block representing a vital phase of the process. The integration of several approaches used in the study may be easily understood thanks to the block diagram's full description of the workflow.

The proposed method uses fractional calculus to design a fractional-order filter for edge detection in color images. The filter is applied to calculate the gradient of the input image. The method that suggested is based on edge detection in both rows and columns. Additionally covered are the EfficientNet model design, model architecture changes, and the transfer-learning method used to train the HAM10000 dataset using ImageNet's pre-trained weights. Better accuracy can be attained by scaling CNNs. It required an iterative manual tweaking operation, either by arbitrary increasing the depth or breadth of the CNNs or by employing a higher input picture resolution. With the goal of finding an appropriate way to scale CNNs for improved accuracy (i.e., model performance) and efficiency (i.e., model parameters), the EfficientNet family of architectures was created by [48].

Normally, to evaluate the performance of various edge detection algorithms, the images are taken, converted into the standard grayscale level of the image and the traditional edge detection algorithms are applied. In this

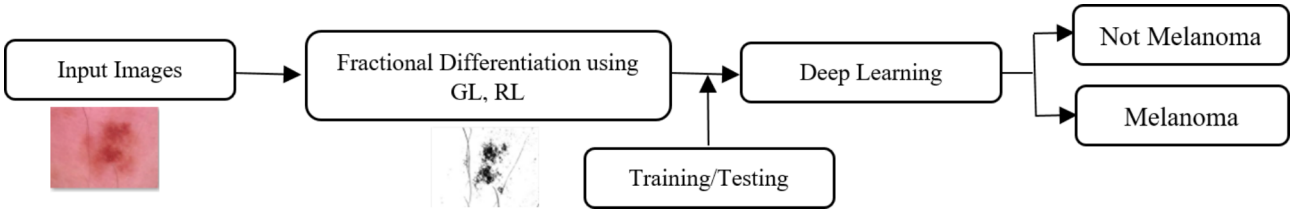

Fig. 1 The general block diagram of the proposed method

paper, six different algorithms are applied: RLR, RLC, GLR, GLC, Sobel, and Canny.

Fractional-order definition

The definitions of fractional calculus that are most frequently used in digital image processing are those offered by Riemann-Liouville and Grunwald-Letnikov [49].

Our research improves edge recognition in skin lesion pictures by applying the G-L equation, a basic tool for fractional differentiation. In order to extract more complex characteristics from the picture data, the G-L equation applies the idea of conventional differentiation to non-integer orders.

The mathematical expression of the G-L equation for fractional differentiation is:

$$D_x^{\alpha}\,[f(x)] = \lim_{h\to 0}\frac{1}{h^{\alpha}}\sum_{k=0}^{\infty}(-1)^k\binom{\alpha}{k}f(x-kh) \quad (1)$$

where $\binom{\alpha}{k}$ are the binomial coefficients.

$$D_x^{\alpha}\,[f(x)] \quad (2)$$

where Eq. (2) is the fractional derivative of the function $f(x)$ with respect to x, and α is the ordered derivative.

Our method involves using the G-L equation on the picture data in order to calculate fractional derivatives, which pick up on small changes in pixel intensities all around the picture. The identification of minute features and boundaries within the skin lesion pictures may be improved by adding fractional differentiation to the edge detection procedure. This improves the overall quality and accuracy of the findings.

Each iteration of the G-L equation takes into account pixel values within the neighborhood indicated by the parameter h as it traverses the picture. A modified picture that better emphasizes critical edge characteristics is produced by iteratively computing fractional derivatives for each pixel.

All things considered, the G-L equation provides a strong mathematical basis for fractional differentiation; this allows us to increase our edge detection skills for better analysis and classification and to extract more information from the skin lesion images.

The R-L equation serves as a fundamental tool for fractional differentiation in our study, enhancing edge recognition in skin lesion pictures. By extending differentiation to non-integer orders, the R-L equation enables a more intricate analysis of picture data.

For fractional differentiation, the mathematical expression of the R-L equation is:

$$D_x^{\alpha}\,[f(x)] = \frac{1}{\Gamma(n-\alpha)}\frac{d^n}{dx^n}\int_0^x (x-t)^{n-\alpha-1}f(t)dt \quad (3)$$

$$D_x^{\alpha}\,[f(x)] \quad (4)$$

where Eq. (4) denotes the fractional derivative of the function f(x) with respect to x, α represents the order of differentiation, and Γ(n) denotes the gamma function.

Applying the R-L equation to skin lesion pictures and computing fractional derivatives enables us to capture the intricate fluctuations in pixel intensities across the image. Adding fractional differentiation to the method enhances the quality and accuracy of edge identification results, enabling better recognition of fine features and boundaries within the images.

The R-L equation operates by integrating pixel values within a specified neighborhood surrounding each picture pixel. This process considers the contributions of nearby pixels to the fractional derivative computation. By computing fractional derivatives for every pixel, this integration technique generates a picture representation that highlights important edge characteristics more clearly.

The R-L equation offers a robust mathematical framework for fractional differentiation, enhancing our edge recognition capabilities and allowing for the extraction of more detailed information from skin lesion images. This facilitates more effective analysis and classification of the images.

Dataset

The HAM10000 dataset and its distribution for training and testing are described in this section.

HAM10000 dataset

The HAM10000 dataset was released by Tschandl et al. in 2018 and is publicly available at [50]. This dataset was created to address challenges in the classification of dermatoscopic images. It consists of 10,015 Red-Green-Blue (RGB) images, collected over a span of 20 years from two distinct medical sources: the Department of Dermatology at the Medical University of Vienna, Austria, and the Cliff Rosendahl in Queensland, Australia. Each image has a resolution of 600×450 pixels and is stored in JPEG format.

This dataset is comprehensive in terms of the diagnostic categories it represents, covering a wide range of pigmented lesions such as actinic keratoses and intraepithelial carcinoma (akiec), basal cell carcinoma (bcc), benign keratosis-like lesions (bkl), dermatofibroma (df), melanoma (mel), melanocytic nevi (nv), and vascular lesions like angiomas and angiokeratomas. The diagnostic categories, illustrated in Fig. 2, are designed to assist computer scientists who may not be familiar with dermatology literature.

Due to its well-organized and representative nature, the HAM10000 dataset has been widely utilized in the field. It served as the primary data source for the ISIC2018

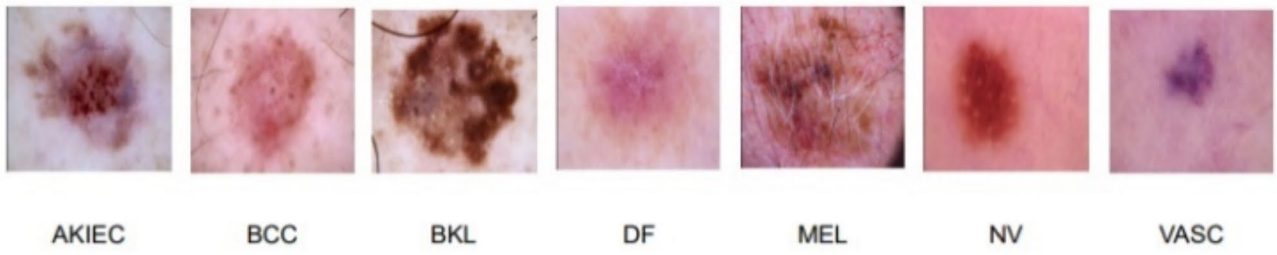

Fig. 2 Example of Skin lesions in HAM10000 dataset [50]

Table 1 Class wise distribution of the HAM10000 dataset

Diagnostic category	Number of images	Training	Testing
nv	6705	6.034	671
mel	1113	1001	112
bkl	1099	989	110
bcc	514	462	52
akiec	327	294	33
vasc	142	127	15
df	115	103	12
Total	10,015	9010	1005

classification challenge and continues to be included in the ongoing ISIC2019 challenge. The distribution of images across each diagnostic category is detailed in Table 1.

In Table 1, the distribution of the HAM10000 dataset by class is depicted, showcasing images classified based on diagnostic criteria. The dataset comprises 10,015 images encompassing a diverse array of dermatological disorders, including melanocytic nevi, melanoma, benign keratosis-like lesions, basal cell carcinoma, actinic keratoses, intraepithelial carcinoma, vascular lesions, and dermatofibroma. Notably, melanocytic nevi constitute the largest category with 6,705 images, followed by melanoma with 1,113 images, and benign keratosis-like lesions with 1,099 images. Additionally, basal cell carcinoma, actinic keratoses, vascular lesions, and dermatofibroma are represented with 514, 327, 142, and 115 images, respectively. The dataset is partitioned into training and testing sets, comprising 9,010 and 1,005 images, respectively, facilitating comprehensive examination and evaluation within the realm of dermatological image classification.

The dataset is publicly available at the following link: https://paperswithcode.com/dataset/ham10000-1.

Dataset organization

The HAM10000 dataset is split into two sections: training (90%) and testing (10%). The testing set assisted in evaluating how well our trained models performed. Regarding the training and testing sets, it was ensured that there were no duplicate images. In Table 1, there are two sets of the HAM10000 dataset's class-wise distribution.

Table 1 provides a detailed breakdown of the class-wise distribution within the HAM10000 dataset. This distribution encompasses seven types of skin cancer, namely akiec, bcc, bkl, df, mel, nv, and vascular lesions. The table showcases the number of images present in each class, offering insights into the dataset's composition and the prevalence of different skin conditions represented within it. The table indicates that 9,010 images are allocated to the training set, with specific counts for each category ranging from 6,034 for nv to 103 for df. Additionally, the testing set comprises 1,005 images, distributed among the diagnostic categories as shown in the table.

Proposed edge detection method

Fractional derivative engine

The first step involves specifying the differential equation to solve, which in this case is the simple $(x)=I\hat{}a\ (x)$ where I is the image and α is the fractional order. Given the digital input, a discrete solution was approximated numerically. Subsequently, functions for RL and GL operations were implemented and optimized. This fractional engine will be used to perform all image processing operations.

Processing HAM10000

The HAM 10,000 images are read and converted to gray-scale. The fractional engine is then used to produce RL (row-wise) and GL (column-wise) operation results at alpha=0.5. Canny and Sobel filters are also applied, and the results are stored in our data store. All the filters are run at default parameters, as detailed in the illustration in Fig. 3.

Efficientnetv2s Architecture

Skin cancer is a major worldwide health problem due to its increasing incidence rate and potential for deadly results if left untreated. Increased survival rates and less strain on healthcare systems are directly correlated with early identification. Deep learning models have demonstrated potential in a number of medical image processing applications, including the diagnosis of skin cancer.

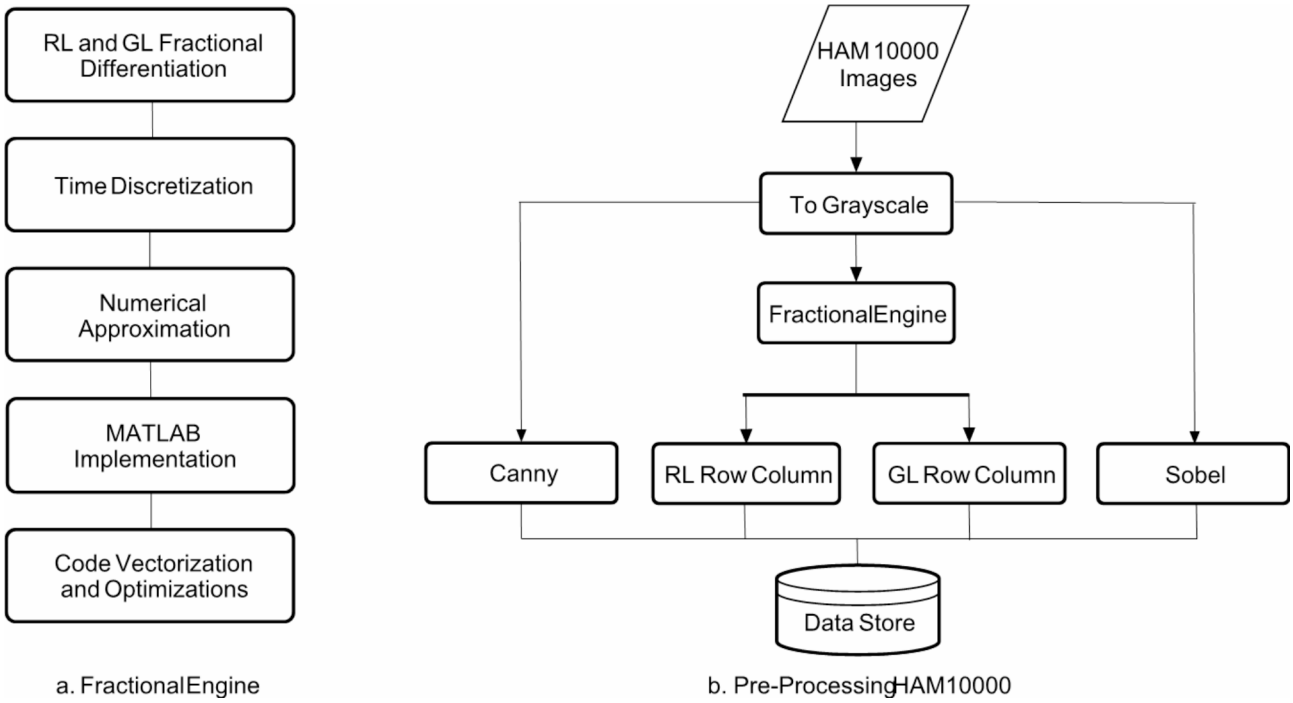

Fig. 3 Block diagrams of the methods employed

With the architecture of EfficientNetV2S, the potential of transfer learning for skin cancer diagnosis is investigated. Transfer learning makes it possible to use the information gained from pre-training on big datasets to improve performance on smaller target datasets and shorten training times. The goal is to improve overall classification accuracy and identify minority classes by optimizing EfficientNetV2S on the HAM10000 dataset and employing class weight methodologies.

The EfficientNetV2S architecture, which has demonstrated exceptional performance across a variety of computer vision workloads, is at the heart of our technique. Starting the model using weights that have already been trained on a sizable dataset (ImageNet) and then refining it on the HAM10000 dataset takes advantage of transfer learning. To mitigate the consequences of data imbalance, class weighting strategies are used that assign more weight to minority classes during model training. With greater attention paid to the underrepresented classes, the model performs better at spotting skin cancer in all classes as a result of this strategy [51].

In Fig. 4, the EfficientNetV2S design is shown in a cohesive fashion, with components (a) and (b) standing for various levels or characteristics of this architecture. Part (a) shows the first few layers of the EfficientNetV2S model, which are in charge of taking in data and extracting fundamental features. These levels include the input layer, convolutional layers, and pooling layers. Part (b), on the other hand, stands for the architecture's subsequent layers or modules, such as dense layers, skip connections, and output layers. These layers combine the retrieved information and provide classifications or predictions. The EfficientNetV2S architecture is shown in Fig. 4 in a unified fashion, which helps to comprehend its design and operational flow better by providing a thorough overview of the model's structure and functional components.

Linear blending (weighted sum)

The study employs linear blending, or weighted sum, to enhance skin lesion categorization precision by applying weights to image components and multiple edge detection algorithms.

Two different weighted-sum configurations are explored. In the first configuration, equal weights are assigned to the original image and the combined edge detection methods, distributing the weight evenly (0.5) among all components. This approach balances edge clarity and overall texture, resulting in enhanced lesion boundaries without losing important details from the original image.

By contrast, the second setup gives the original picture a larger weight of 0.8 and gives the edge detection components a combined weight of 0.2. Thanks to this setup, we can boost classification accuracy significantly while keeping the original image's fundamental elements intact and making use of improved edge detection.

The research shows that a weighted combination of initial pictures and improved edge detection methods

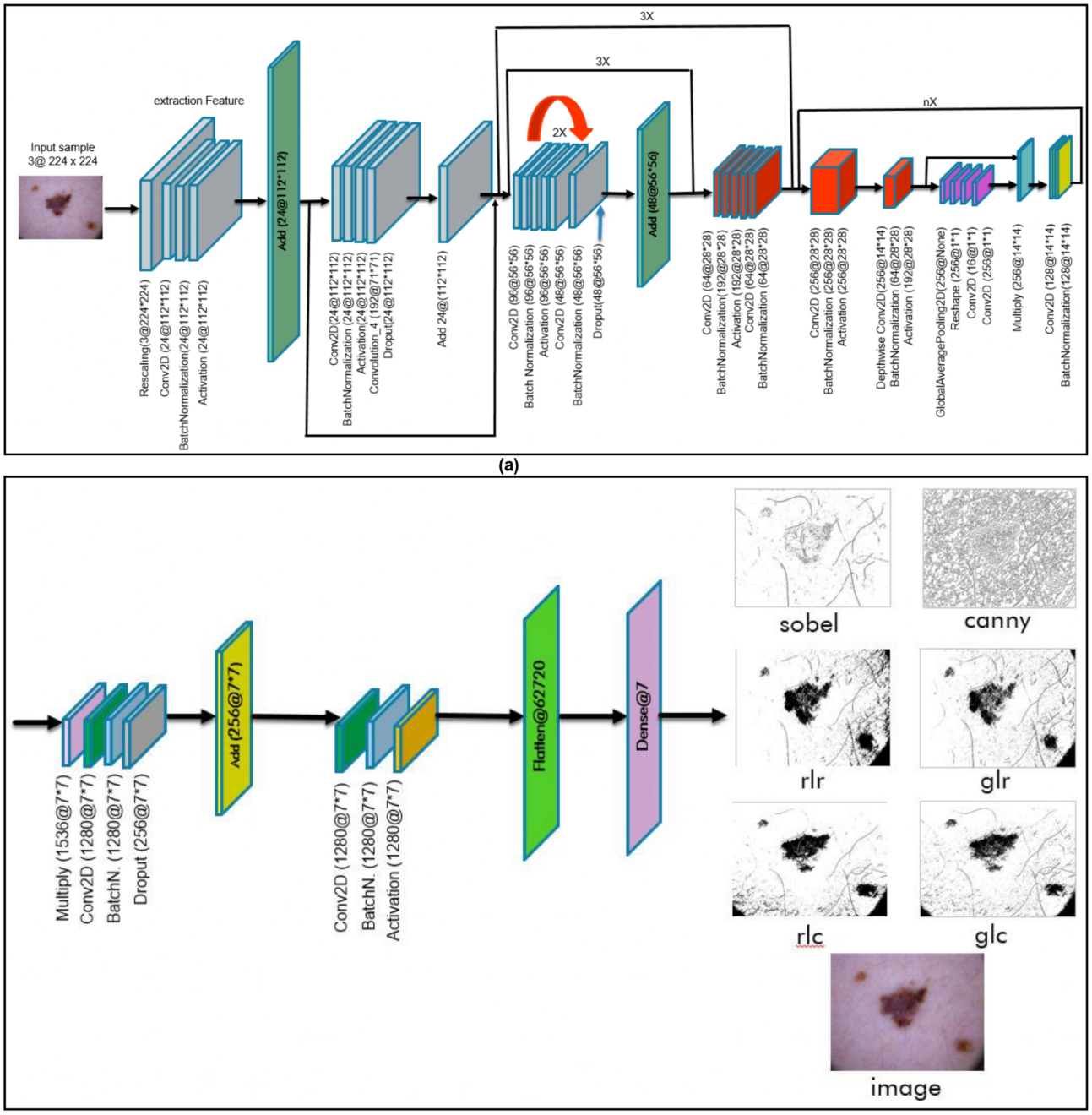

Fig. 4 **(a)** and **(b)** Block diagrams related to proposed method

enhances the model's generalizability and accuracy in labeling skin lesions.

Weighted sum is a mathematical operation that combines image pixel values using specific weights, commonly used for enhancement and filtering techniques. It multiplies each pixel's weight and sums them [52].

$$g\left(x\right)=\left(1-\alpha\ \right)f0\left(x\right)+\alpha\,\mathrm{f1}\left(\mathrm{x}\right) \tag{5}$$

The weighted sum equation is a basic tool for combining various picture components in our investigation. In this case,

$f0(x)$ and $f1(x)$ are two separate functions or representations of images, and α is a weighting parameter that decides how much each function contributes to the final blended output $g(x)$. When the value of α is zero, the function (x) largely reflects $f0(x)$, whereas $f1(x)$ does not affect the outcome. Alternatively, if α is equal to 1,

then (x) replicates $f1(x)$, but $f0(x)$ becomes insignificant. The equation determines the degree to which each function contributes by interpolating between $f0$ (x) and $f1$ (x) for values of α between 0 and 1. This interpolation algorithm provides a flexible method for mixing, morphing, and filtering images, among other areas of image processing.

Our work improves skin lesion picture classification accuracy by utilizing the weighted sum equation and edge detection algorithms. Composite images are generated, balancing original image characteristics with edge enhancements. The model's accuracy is enhanced by meticulous selection of α values. The weighted sum equation is used to compare original images with different edge detection output configurations, systematically exploring the impact of different emphasis on edge detection characteristics.

The weighted sum equation enhances skin lesion analysis classification accuracy by integrating picture components, providing a versatile approach to medical image analysis tasks.

A weighted sum has been calculated for both RL and GL, representing horizontal and vertical edge detectors, to create a combined matrix of the four edge detectors. Moreover, a weighted sum has been computed between the combined matrix and the original image using varying addition factors (degrees of blending), as illustrated in Table 2.

Experimental results

Images of skin cancer were used to conduct and test the experiment to using the fractional differentiator to obtain the clean edge map. Here, a variety of experiments have been conducted with and without a noisy environment in order to identify and extract edges. Figure 5 displays the outcomes from using several edge detection algorithms on the original picture displayed after applying 0.5 differentiation in both directions (row and column).

Experiments based on the HAM10000 dataset are performed in order to compare fractional differentiation based on the images. In Fig. 5, the visual results of applying various edge detection techniques to the original image and the experiment are presented.

Network reconstruction edge detection algorithm

CNNs is a neural network that feeds data forward. Its artificial neurons can react to the nearby units of partial coverage, perform well for massive image processing, and seek accuracy and speed by recreating network structures such as CNNs is a neural network that feeds data forward. Its artificial neurons perform well for processing huge images, seek accuracy and speed by recreating network structures, and may react to the surrounding units of a partial coverage [49] such as EfficientNetV2S.

In this paper, a neural network, EfficientNetV2S, is implemented to classify skin cancer images. EfficientNetV2S is a state-of- the art feature extractor that is trained on the ImageNet dataset. The main components and architecture of the proposed approach are described in Fig. 4.

A weighted sum has been applied to both G-L and R-L with alpha equal to 0.5, multiplied by the values of both detected edge pixels. Subsequently, a weighted sum is applied between the total image and the original image, with alpha equaling 0.5 for both total and original images, and another weighted sum is applied, multiplying the total image pixels by 0.2 and the original image pixels by 0.8.

Figure 6 displays the visual outcomes of various edge detection and enhancement approaches on skin cancer images, showcasing their successful identification of lesion borders.

The original skin cancer image is compared with Sobel and Canny edge detection algorithms, resulting in improved visibility of edges, with Sobel producing more distinct edges and Canny reducing breakage.

Techniques for fractional calculus Image improvements with more texture characteristics and well-defined edges are produced by RLc+RLr and GLc+GLr, respectively, by using the Grunwald-Letnikov and Riemann-Liouville criteria. Images enhanced using RLc+RLr have a balanced enhancement, keeping more texture features, but those treated with GLc+GLr have well-defined edges and little noise.

The graphic shows pictures resulting from a weighted sum algorithm, balancing edge clarity and texture. The most noticeable improvement is seen when the original image is given a larger weight, enhancing lesion border visibility without compromising image quality.

The study demonstrates that combining original images with classical and fractional calculus-based edge detection methods enhances the visibility of lesion borders, making skin cancer images more useful for diagnosis. The proposed technique, based on a study on a skin

Table 2 Performance results after applying Weighted Sum

image_type	Training loss	Training Accuracy	Test loss	Test Accuracy	F1 score
(Weighted Sum (total, 0.5) 'glc + glr + 'rlc + rlr + Original Image '	0.3615	9658	7.2377	0.7944	0,79
(Weighted Sum (total, 0.2, original_image, 0.8) 'glc + glr + 'rlc + rlr + Original Image '	0.2358	0.9621	5.3341	0.8104	0,81

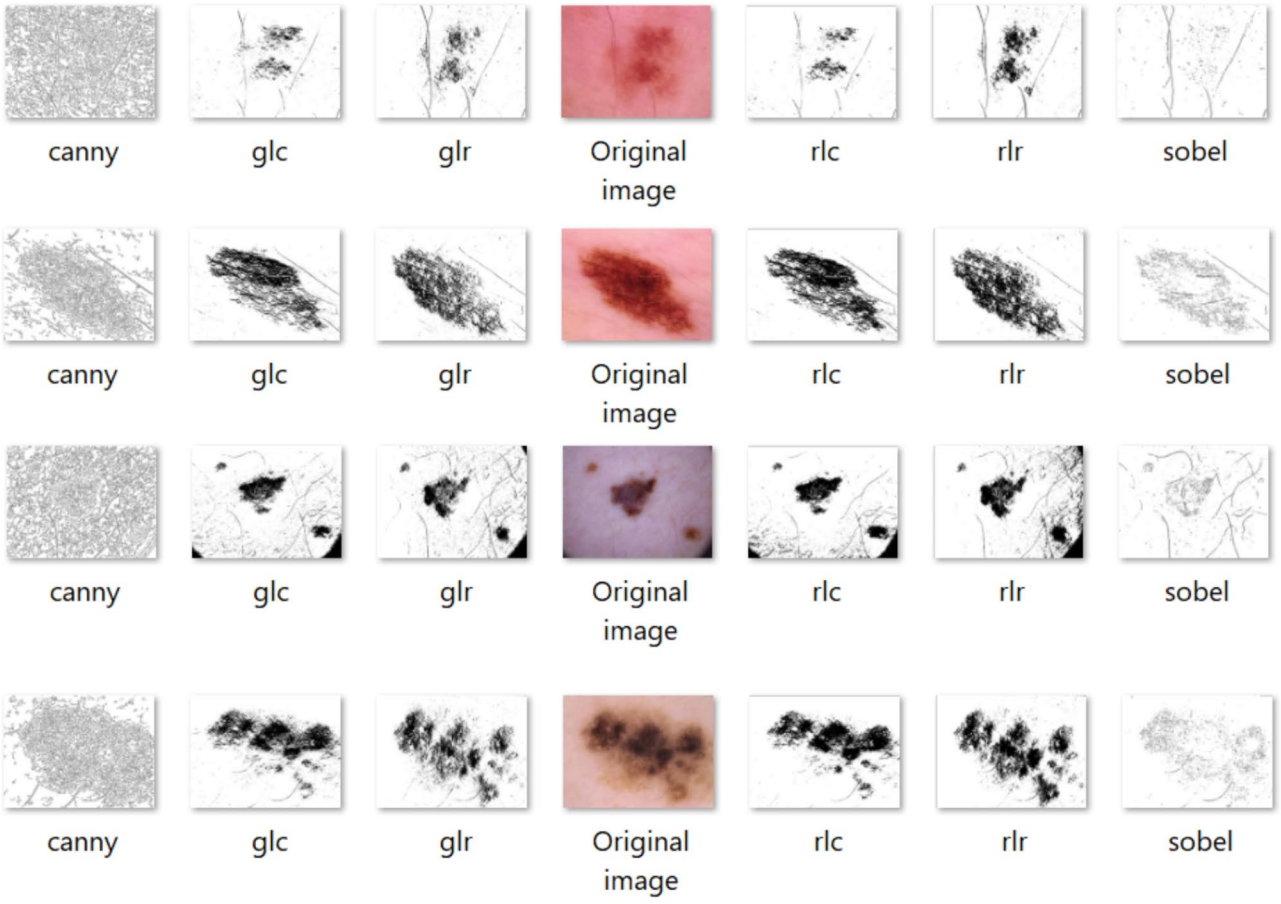

Fig. 5 Sample images used and obtained from fractional differentiations

cancer lesion, uses various image processing techniques to reveal detailed borders and contours, making it easier to spot abnormal areas, and emphasizes edges while reducing noise interference.

The study explores enhanced image edge detection using fractional derivatives of Grunwald-Letnikov and Riemann-Liouville. The method, which can be implemented individually or in tandem, allows for picture analysis beyond traditional limitations and improves visual quality, with encouraging results.

Table 3 presents the results of various edge detection methods for skin cancer pictures. Sobel's moderate training loss and equal accuracy suggest overfitting or training process concerns, while Canny's training accuracy and test accuracy are lower but stronger, with a higher test loss indicating stronger generalization. The G-L criteria method achieves training accuracy of 0.9424 and loss of 0.4798, indicating strong learning and excellent generalization to unseen data. The R-L criteria approach achieves training accuracy of 0.9042 and reasonable test performance with test loss of 6.4744 and F1 score of 0.77. Edge detection approaches improve model durability and accuracy.

GLr+GLc provided the greatest overall performance, indicating its excellent generalization potential; other advanced edge detection approaches, such as RLr+RLc and GLr+GLc, show a better balance between the training and testing phases.

Table 2 shows a weighted sum approach for improving classification performance on skin cancer pictures. The model achieved a training accuracy of 96.58% with a training loss of 0.3615, using a total weight of 0.2 for all components and 0.8 for the original image. This approach combines edge detection approaches with the original image.

The study found that combining edge detection techniques with the original image can improve the model's generalizability to fresh data. In a second setup, the original picture had a heavier weight, resulting in a higher training accuracy of 96.21% and a lower training loss of 0.2358. This approach led to optimal training and test performance, reducing overfitting and increasing the model's resilience.

The weighted sum technique enhances classification outcomes by adding additional weight to the original image, suggesting that the optimal approach is to

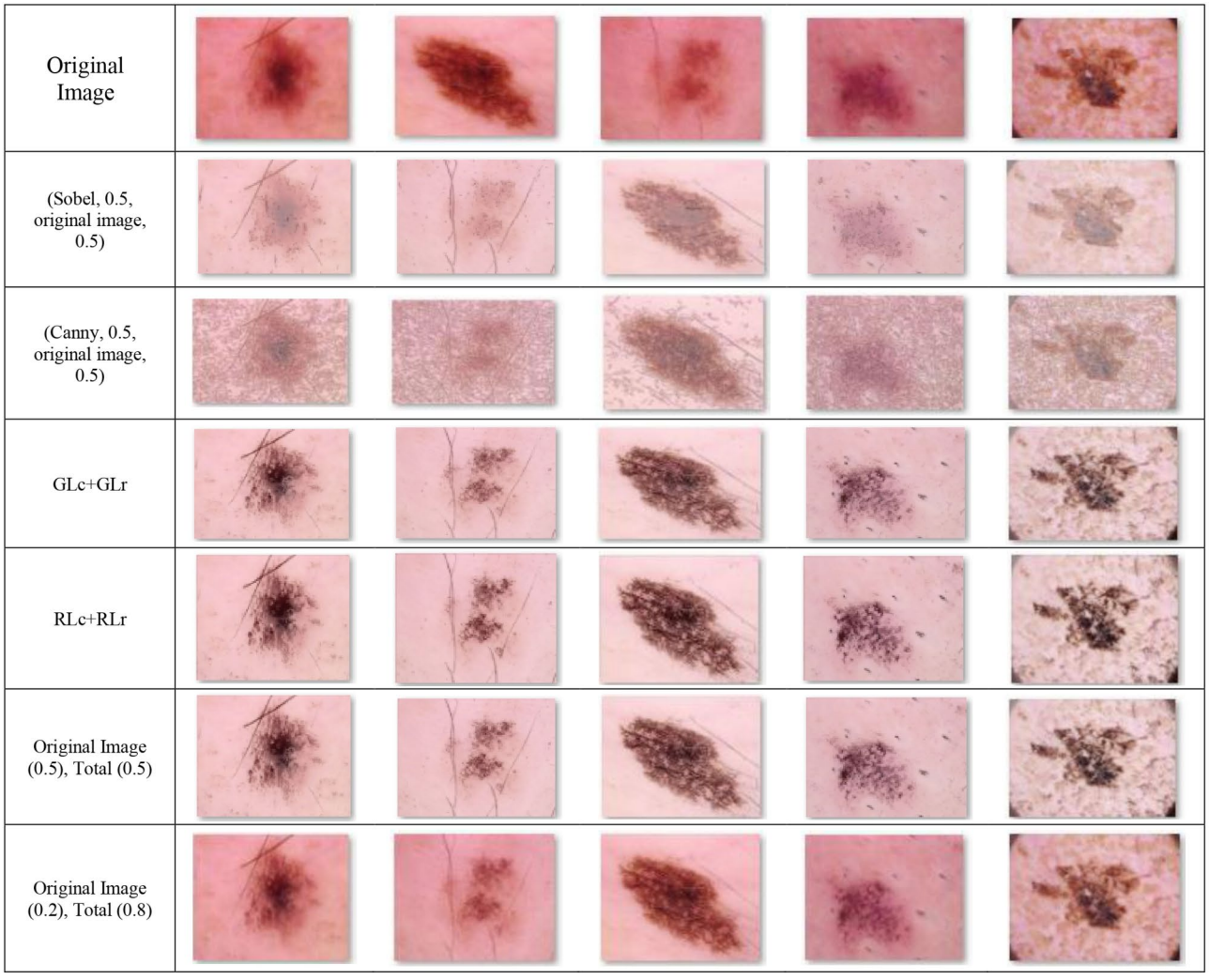

Fig. 6 Original skin cancer image with sobel (original image), Canny (original image), and Fractional Calculus (GLc, GLr), (RLc, RLr), and (GLc, GLr + RLc, RLr) by applying 0.5 differentiation in both directions (row and column)

Table 3 Performance metrics of several edge detection approaches on images of skin cancer with and without noise

image_type	Training loss	Training Accuracy	Test loss	Test Accuracy	F1 score
(Sobel, 0.5, original_image, 0.5)	0.3195	0.3195	8.4766	0.7794	0,77
(Canny, 0.5, original_image, 0.5)	0.4973	0.9132	5.5792	0.7515	0.75
Glr + GLc	0.4798	0.9424	7.4650	0.7764	0,77
RLr + RLc	0.7527	0.9042	6.4744	0.7715	0,77
Original Image	0.3195	0.9605	8.4766	0.7794	0,77

retain more information and incorporate edge detection features.

Discussion

This part examines the findings, draws comparisons to other studies, and showcases the results produced by deep learning models on the HAM10000 dataset. The performance of previous attempts using deep learning models is reviewed to set the stage and establish standards.

According to Table 4, EfficientNetV2S outperforms other CNNs architectures with an accuracy of 81.04%, outperforming Xception, DenseNet-201, Inception-ResNet-V2, GoogLeNet-Places365, AlexNet, and GoogLeNet. It also outperforms MobileNet-V2, with an accuracy of 80.59%. EfficientNetV2S is effective in picture categorization tasks, with ResNet-101 achieving the highest accuracy of 83.99%, making it a strong contender in image classification tasks.

Table 4 Comparison of EfficientNetV2S with other CNNs [53]

CNNs	Accuracy
Xception	78.45
DenseNet-201	78.59
IncpetionResNet-V2	79.39
GoogLeNet-Places365	79.45
GoogLeNet	79.45
AlexNet	79.65
MobileNet-V2	80.59
EfficientNetV2S	81.04
ResNet-50	81.12
ResNet-101	83.99

Table 5 Comparisons between prior work

Paper	Method	Accuracy
[54]	MobileNet	78.54%
[55]	DenseNet201	73.5%
[56]	VGGNet	78%
Proposed Model	EfficientNetV2S	81.04%

Table 5 illustrates how the EfficientNetV2S model compares to other studies that have used the HAM10000 dataset and various approaches for skin lesion categorization. The results demonstrate that EfficientNetV2S achieves the highest accuracy at 81.04%, surpassing previous research's accuracies.

The study compares DenseNet201, MobileNet, and VGGNet models for skin lesion classification accuracy. DenseNet201 has a 73.5% accuracy rate, while MobileNet has a 78.5% rate. VGGNet has a 78% accuracy rate. The EfficientNetV2S model outperforms all combined techniques due to its innovative architecture and feature-leveraging capabilities, offering a robust solution.

The proposed edge detection enhancements improve performance and strengthen representations of skin lesions in images. Experimental setups and deep learning training may enhance performance. Fractional derivatives are effective in edge detection, extracting geometric information better than other texture identifiers. Future work could integrate fractional derivatives with texture identifiers.

Conclusion

The advancement in image processing leads to the application of edge detectors in feature detection or feature extraction. Edge detectors are more important because they provide a lot of information about the geometry of the objects in the scene. The paper proposes the use of fractional derivatives, a non-integer differentiation implementation of the Grunwald-Letnikov definition, for image enhancement in the automatic detection of melanoma. Two approaches that use the Grunwald-Letnikov definition are developed and evaluated. The Grunwald-Letnikov (G-L) and Riemann-Liouville (R-L) definitions derive the equation at the given order of derivative, which is the main asset of the two developed algorithms. Then, the derivatives are added to the original images for enhancement. Furthermore, the deep learner classifies the enhanced images. The proposed methodology is adapted for automatic malignant melanoma detection, which is a recent problem in medical imaging. The system achieves an encouraging and comparable rate of 81.04% recognition accuracy. The results show that the proposed technique achieves inspiring results and is open to further development.

Limitations and future works

The paper proposes a fractional derivative-based image enhancement for improved automatic melanoma detection. The experiments are done on the dataset. The system undergoes training on a single dataset, which poses a significant limitation. Therefore, it is limited by the variations of this dataset and also inherits errors from the dataset. The study's expert classification of the images provided in the dataset is another limitation. As a result, these two points—obtaining datasets that sufficiently cover all types of samples and labeling with expert opinions—are general limitations of such systems.

There are some future directions in which a researcher can improve the system proposed in this paper. One of them is to use all the fractions of the derivative and combine them. Another clear direction we can identify is the fusion of fractional derivative information with texture information. Thus, having a robust geometric representation using fractional derivatives in the proposed way and a well-performing texture identifier (e.g., LBP) can even improve the robustness of the representations.

Acknowledgements

We would like to express our gratitude to Cyprus International University administration that supports our study to make it possible.

Author contributions

Conceptualization, B.A,. and K.Y.; methodology, B.A. and K.Y.; software, B.A.; validation B.A. and K.Y.; formal analysis, B.A. and K.Y.; resources, B.A. and K.Y.; data curation, B.A. and K.Y.; writing—original draft preparation, B.A.; writing—review and editing, B.A. and K.Y.; visualization, B.A. and K.Y.; supervision, B.A. and K.Y.; project administration, B.A. and K.Y.

Funding

Not Applicable.

Data availability

The used data was taken from the reference [37]. The dataset is publicly available in the following link. https://paperswithcode.com/dataset/ham10000-1.

Declarations

Ethical approval

Not Applicable.

Informed consent

Not Applicable.

Consent for publication
Not Applicable.

Competing interests
The authors declare no competing interests.

Received: 2 March 2024 / Accepted: 14 August 2024
Published online: 02 September 2024

References

1. Shashi P, R S. Review study on Digital Image Processing and Segmentation. Am J Comput Sci Technol. 2019;2(4):68. https://doi.org/10.11648/j.ajcst.20190204.14.
2. Shafiabadi M, Kamkar-Rouhani A, Ghavami Riabi SR, Kahoo AR, Tokhmechi B. Identification of reservoir fractures on FMI image logs using Canny and Sobel edge detection algorithms. Oil Gas Sci Technol. 2021;76. https://doi.org/10.2516/ogst/2020086.
3. Chen G, Jiang Z, Kamruzzaman MM. Radar remote sensing image retrieval algorithm based on improved Sobel operator. J Vis Commun Image Represent. 2020;71:102720. https://doi.org/10.1016/j.jvcir.2019.102720.
4. Journal I, Creative OF. Edge Detection Algorithms on Digital Signal Processor Dm642. Int J Creat Res THOUGHTS no Oct, 2020.
5. Fisher Y. ConvUNeXt [14]. ScienceDirect, 1995.
6. Ansari MY, Chandrasekar V, Singh AV, Dakua SP. Re-Routing Drugs to Blood Brain Barrier: A Comprehensive Analysis of Machine Learning Approaches With Fingerprint Amalgamation and Data Balancing, *IEEE Access*, 2023;11(February):9890–9906, https://doi.org/10.1109/ACCESS.2022.3233110
7. Ansari MY, Qaraqe M, Charafeddine F, Serpedin E, Righetti R, Qaraqe K. Estimating age and gender from electrocardiogram signals: a comprehensive review of the past decade. Artif Intell Med. 2023;146:102690. https://doi.org/10.1016/j.artmed.2023.102690.
8. Ansari MY, Qaraqe M. MEFood: A Large-Scale Representative Benchmark of Quotidian Foods for the Middle East, IEEE Access, 2023;11(January):4589–4601, https://doi.org/10.1109/ACCESS.2023.3234519
9. Mohammed AA, Al-irhayim YF. gender of speakers, 2021;26(1):101–107.
10. El FDE, Deep Learning for Skin Lesion Classification. Augment, train, and Ensemble Aprendizado Profundo para Classifica , c ˜ Ao De Les ˜ Oes De Pele : Aumento, Treino E Conjunto Deep Learning for skin lesion classification. Augment, Train, and Ensemble Ap; 2019.
11. Codella NCF, et al. Skin lesion analysis toward melanoma detection: a challenge at the 2017 International symposium on biomedical imaging (ISBI), hosted by the international skin imaging collaboration (ISIC). Proc - Int Symp Biomed Imaging. 2018;2018–April(no Isbi):168–72. https://doi.org/10.1109/ISBI.2018.8363547.
12. Grignaffini F, et al. Anomaly detection for skin lesion images using convolutional neural network and injection of handcrafted features: a method that bypasses the preprocessing of dermoscopic images. Algorithms. 2023;16(10). https://doi.org/10.3390/a16100466.
13. Wu Y, Chen B, Zeng A, Pan D, Wang R, Zhao S. Skin Cancer Classification With Deep Learning: A Systematic Review, Front. Oncol., 2022;12(July):1–20, https://doi.org/10.3389/fonc.2022.893972
14. Hill GD, Bellekens XJA. Deep Learning Based Cryptographic Primitive Classification, pp. 1–9, 2017, [Online]. Available: http://arxiv.org/abs/1709.08385
15. Cheong KH, et al. An automated skin melanoma detection system with melanoma-index based on entropy features. Biocybern Biomed Eng. 2021;41(3):997–1012. https://doi.org/10.1016/j.bbe.2021.05.010.
16. Han Z, Jian M, Wang GG. ConvUNeXt: an efficient convolution neural network for medical image segmentation. Knowledge-Based Syst. 2022;253:109512. https://doi.org/10.1016/j.knosys.2022.109512.
17. Ansari MY, et al. A lightweight neural network with multiscale feature enhancement for liver CT segmentation. Sci Rep. 2022;12(1):1–12. https://doi.org/10.1038/s41598-022-16828-6.
18. Le Lay L, Oustaloup A, Levron F, Trigeassou J-C. Frequency Identification by Non Integer Model, IFAC Proc. Vol., 1998;31(18):281–286, https://doi.org/10.1016/s1474-6670(17)42005-2
19. Mu'lla MAM. Fractional Calculus, fractional Differential equations and applications. OALib. 2020;07(06):1–9. https://doi.org/10.4236/oalib.1106244.
20. Xie Y, Zhang J, Shen C, Xia Y. CoTr: efficiently bridging CNN and Transformer for 3D medical image segmentation. Lect Notes Comput Sci (Including Subser Lect Notes Artif Intell Lect Notes Bioinformatics). 2021;12903:171–80. https://doi.org/10.1007/978-3-030-87199-4_16. LNCS.
21. Ansari MY, et al. Practical utility of liver segmentation methods in clinical surgeries and interventions. BMC Med Imaging. 2022;22(1):1–17. https://doi.org/10.1186/s12880-022-00825-2.
22. Akhtar Y, et al. Risk Assessment of computer-aided Diagnostic Software for hepatic resection. IEEE Trans Radiat Plasma Med Sci. 2022;6:667–77. https://doi.org/10.1109/TRPMS.2021.3071148.
23. Rai P, et al. Efficacy of fusion imaging for immediate post-ablation assessment of malignant liver neoplasms: a systematic review. Cancer Med. 2023;12(13):14225–51. https://doi.org/10.1002/cam4.6089.
24. Ansari MY, et al. Advancements in Deep Learning for B-Mode Ultrasound Segmentation: a Comprehensive Review. IEEE Trans Emerg Top Comput Intell. 2024;8(3):2126–49. https://doi.org/10.1109/TETCI.2024.3377676.
25. Sparavigna AC. Fractional differentiation based image processing. Collerdio Univ. 2015;1–7. https://doi.org/10.48550/arXiv.0910.2381.
26. Sun Y, Zeng Z, Song J. Existence and uniqueness for the boundary value problems of nonlinear fractional Differential equation. Appl Math. 2017;08(03):312–23. https://doi.org/10.4236/am.2017.83026.
27. Takayasu H. Fractals inthe physical sciences. Manchester University Press Oxford Road; 1990.
28. Hertzmann A, Jacobs CE, Oliver N, Curless B, Salesin DH. Image analogies. Proc 28th Annu Conf Comput Graph Interact Tech SIGGRAPH 2001. 2001;(August):327–40. https://doi.org/10.1145/383259.383295.
29. Drakopoulos V. Fractal-based image encoding and compression techniques. Commun - Sci Lett Univ Žilina. 2013;15(3):48–55. https://doi.org/10.26552/com.c.2013.3.48-55.
30. Awrejcewicz J, Papkova IV. Introduction to Fractal Dynamics. ResearchGate. 2016;no January:14–30. https://doi.org/10.1142/9789814719704_0002.
31. Fisher Y. Quadtrees. Springer-Verlag New York, pp. 55–6, 1995.
32. Mandelbrot BB, Wheeler JA. The Fractal geometry of Nature. Am J Phys. 1983;51:286–7. https://doi.org/10.1119/1.13295. no. 3.
33. Emre Celebi M, Wen Q, Iyatomi H, Shimizu K, Zhou H, Schaefer G. A state-of-the-art survey on lesion border detection in dermoscopy images. Dermoscopy Image Anal. 2015;97–130. https://doi.org/10.1201/b19107.
34. Hosny KM, Elshoura D, Mohamed ER, Vrochidou E, Papakostas GA. Deep Learning and Optimization-Based Methods for Skin Lesions Segmentation: A Review, IEEE Access, 2023;11(July):85467–85488, https://doi.org/10.1109/ACCESS.2023.3303961
35. Canny J. A Computational Approach to Edge Detection. IEEE Trans Pattern Anal Mach Intell. 1986;8:PAMI. https://doi.org/10.1109/TPAMI.1986.4767851.
36. Amer GMH, Abushaala AM. Edge detection methods. 2015 2nd World Symp Web Appl Netw WSWAN 2015. 2015;1–7. https://doi.org/10.1109/WSWAN.2015.7210349.
37. Tan M, Le QV. EfficientNetV2: Smaller Models and Faster Training, Proc. Mach. Learn. Res., 2021;139:10096–10106.
38. Marr D, Hildreth E. Theory of edge detection, Proc. R. Soc. London - Biol. Sci., 1980;207(1167):187–217, https://doi.org/10.1098/rspb.1980.0020
39. Langdon J. The perception of three-dimensional solids. Q J Experimental Psychol. 1955;7:133–46. https://doi.org/10.1080/17470215508416686. no. 3.
40. Stocks N. 済無No Title No Title No Title. IEEE. no. 2016;206:1–23.
41. Kalra A, Chhokar RL. A hybrid approach using sobel and canny operator for digital image edge detection. Proc - 2016 Int Conf Micro-Electronics Telecommun Eng ICMETE 2016. 2016;305–10. https://doi.org/10.1109/ICMETE.2016.49.
42. Cui S, Wang Y, Qian X, Deng Z. Image Processing techniques in Shockwave Detection and modeling. J Signal Inf Process. 2013;04(03):109–13. https://doi.org/10.4236/jsip.2013.43b019.
43. Engel K, Hadwiger M, Kniss JM, Lefohn AE, Weiskopf D. SIGGRAPH 2004 Notes: Real-Time Volume Graphics.
44. Mustafa ZA, Abrahim BA, Omara A, Mohammed AA, Hassan IA, Mustafa EA. Reduction of Speckle noise and image enhancement in Ultrasound Image using filtering technique and edge detection. J Clin Eng. 2020;45(1):51–65. https://doi.org/10.1097/jce.0000000000000378.
45. Maji SK, Yahia HM, Badri H. Reconstructing an image from its edge representation. Digit Signal Process Rev J. 2013;23:1867–76. https://doi.org/10.1016/j.dsp.2013.06.013.
46. Ali K, Shaikh ZA, Khan AA, Laghari AA. Multiclass skin cancer classification using EfficientNets – a first step towards preventing skin cancer. Neurosci Inf. 2022;2(4):100034. https://doi.org/10.1016/j.neuri.2021.100034.
47. Behara K, Bhero E, Agee JT. An improved skin lesion classification using a Hybrid Approach with active Contour Snake Model and Lightweight

attention-guided Capsule Networks. Diagnostics. 2024;14(6). https://doi.org/10.3390/diagnostics14060636.
48. Lehtomäki M, et al. Object classification and Recognition from Mobile Laser scanning point clouds in a Road Environment. IEEE Trans Geosci Remote Sens. 2016;54(2):1226–39. https://doi.org/10.1109/TGRS.2015.2476502.
49. Lopez-Molina C, Bustince H, De Baets B. Separability criteria for the evaluation of Boundary Detection Benchmarks. IEEE Trans Image Process. 2016;25(3):1047–55. https://doi.org/10.1109/TIP.2015.2510284.
50. Tschandl P, Rosendahl C, Kittler H. Data descriptor: the HAM10000 dataset, a large collection of multi-source dermatoscopic images of common pigmented skin lesions. Sci Data. 2018;5:1–9. https://doi.org/10.1038/sdata.2018.161.
51. Yang Q, Chen D, Zhao T, Chen Y. Fractional calculus in image processing: a review. Fract Calc Appl Anal. 2016;19(5):1222–49. https://doi.org/10.1515/fca-2016-0063.
52. Chaikan P, Mitatha S, Improving the Addweighted Function in OpenCV 3.0 Using SSE and, Intrinsics AVX. Int. J. Eng. Technol., 2017;9(1):45–49, https://doi.org/10.7763/ijet.2017.v9.943
53. Nguyen HH, Chan CW. Multiple neural networks for a long term time series forecast. Neural Comput Appl. 2004;13:90–8.
54. Innani S, Dutande P, Baheti B, Baid U, Talbar S. Deep learning based novel cascaded approach for skin lesion analysis. In: Communications in computer and information science. vol. 1776. 2023. p. 615–26. https://doi.org/10.1007/978-3-031-31407-0_46.
55. Fraiwan M, Faouri E. On the automatic detection and classification of skin cancer using deep transfer learning. Sensors. 2022;22(13):4963. https://doi.org/10.3390/s22134963.
56. Thurnhofer-Hemsi K, Domínguez E. A convolutional neural network framework for accurate skin cancer detection. Neural Process Lett. 2021;53(5):3073–93. https://doi.org/10.1007/s11063-020-10364-y.

Publisher's note